The Impact of Spatial Self-Shielding on Pin-Wise Reaction Rates

William Boyd, Benoit Forget, Kord Smith

Massachusetts Institute of Technology, Department of Nuclear Science and Engineering, 77 Massachusetts Avenue, Building 24, Cambridge, MA 02139, United States

Abstract

Keywords: Multi-group cross-sections, spatial homogenization, spatial self-shielding

1. Introduction

The nuclear reactor physics community has long strived for deterministic neutron transport-based tools for whole-core reactor analysis. A key challenge for whole-core multi-group transport methods is accurate reactor agnostic multi-group cross section (MGXS) generation. The MGXS generation process applies a series of approximations to produce spatially homogenized and energy condensed MGXS in each spatial zone and energy group. ... However, the practical impact of ... is less understood. This paper investigates the ... and quantifies its significance for heterogeneous PWR problems.

This work employs Monte Carlo (MC) neutron transport simulations to generate MGXS. Monte Carlo methods have increasingly been used to generate few group constants for coarse mesh diffusion, most notably by the Serpent MC code (Leppänen, 2013), and to a much lesser extent, for high-fidelity neutron transport methods (Redmond, 1997; Nelson, 2014; Cai, 2014; Boyd, 2016). The advantage of a MC-based approach is that all of the relevant physics are directly embedded into MGXS by weighting the continuous energy cross sections with a statistical proxy to the "true" neutron flux.

This paper seeks to identify the bias between continuous energy and multi-group transport methods for MGXS libraries which account for spatial self-shielding effects[1] to varying degrees. In particular, this paper quantifies the difference in the approximation error between simulations in which the same MGXS are used in each unique fuel pin (*e.g.*, each fuel enrichment) and those in which unique MGXS are used in each and every pin. The former case does little if anything to model spatial self-shielding effects, whereas the latter case "fully" resolves these effects, albeit at the expense of very large MGXS libraries.

The content in this paper is organized as follows. Two different schemes for spatial homogenization of pin-wise MGXS are introduced in Sec. 2. The need for a new, more flexible and specialized approach to spatial homogenization which appropriately captures spatial self-shielding effects with minimal computational expense is discussed in Sec. 5.

2. Methodology

2.1. Continuous Energy Calculations with OpenMC

-OpenMC Romano and Forget (2013) -Python API Boyd et al. (2016a) -NNDC data National Nuclear Data Center, Brookhaven National Laboratory (2016) -distribcell tallies Lax et al. (2014) -`openmc.mgxs` -tallied in CASMO's seventy energy group structure Rhodes et al. (2006) -iso-in-lab -runtime parameters: -num. particles, batches -computer hardware

2.2. Multi-Group Calculations with OpenMOC

-OpenMOC Boyd et al. (2014) -multi-core parallelism Boyd et al. (2016b) -runtime parameters: -azim angles, spacing -num. FSRs -CMFD energy and spatial mesh -computer hardware

2.3. Pin-wise Spatial Homogenization Schemes

-focus less on introducing these as "schemes" per se -rather two spatial self-shielding models to quantify approx. error

This paper employs two different spatial homogenization schemes to model spatial self-shielding effects in MGXS. Although all spatial zones may experience spatial self-shielding, this chapter only models the impact of spatial self-shielding on MGXS in fissile regions. The null and degenerate spatial homogenization schemes are introduced in Sec. 2.3.1 and Sec. 2.3.2, respectively. These schemes model spatial self-shielding for each fuel pin with increasing granularity and complexity. A fuel assembly and 2×2 colorset with reflector model are color-coded by material and illustrated in Fig. 1 for each homogenization scheme.

The `openmc.mgxs` module was used to compute 70-group MGXS with OpenMC for both the assembly and colorset benchmarks. The tallied MGXS data was condensed to coarse 2-group and 8-group structures with downstream data processing as necessary. The OpenMC simulations were performed with 1000 batches with 10^6 particle histories per batch for each benchmark. Stationarity of the fission source was obtained with 100 inactive batches for each benchmark. OpenMC's "iso-in-lab" feature was employed to enable consistent comparisons between OpenMC's reference results and OpenMOC's calculations with an isotropic in lab scattering source.

Email addresses: wboyd@mit.edu (William Boyd), bforget@mit.edu (Benoit Forget), kord@mit.edu (Kord Smith)

[1] The effects of neighboring pins, burnable poisons, reflectors and the core baffle are each of interest in the context of spatial self-shielding.

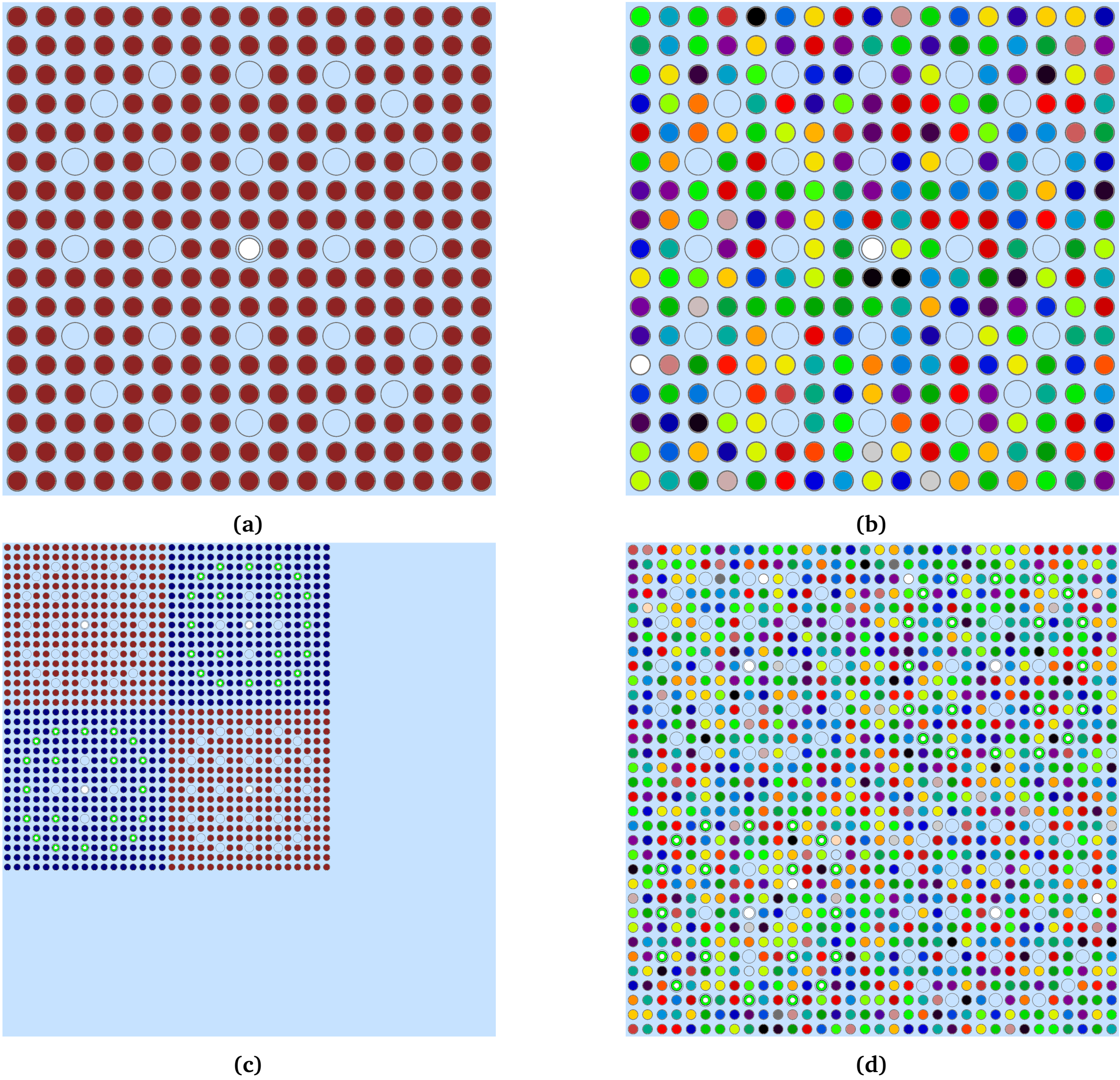

Figure 1. OpenMOC materials for the (a)-(b) assembly and (c)-(d) 2×2 colorset models with null and degenerate homogenization, respectively.

2.3.1. Null Homogenization

The *null* spatial homogenization scheme uses a single Monte Carlo calculation of the complete heterogeneous geometry to generate MGXS for each material. In this way, the null scheme fully abandons the multi-level approach used by most traditional approaches to generate MGXS. The spatially self-shielded flux is used to collapse the cross sections in each material with a unique isotopic composition. The null scheme does not account for spatial self-shielding effects experienced by different fuel pins filled by the same type of fuel, and instead averages these effects across the entire geometry. A single MGXS is employed in each instance of a material zone, such as a fuel pin replicated many times throughout a benchmark geometry.

2.3.2. Degenerate Homogenization

Unlike the null spatial homogenization scheme, the *degenerate* scheme accounts for the different spatial self-shielding effects experienced by each instance of each fuel pin throughout a heterogeneous geometry. Like the null scheme, a single MC calculation of the complete heterogeneous geometry is used to generate MGXS for all materials. Unlike the null scheme, the MGXS are tallied separately for each instance of fissile material zones. For example, if a heterogeneous benchmark includes N fuel pins, then N collections of MGXS are separately tabulated for each fuel pin instance. The degenerate scheme tallies different MGXS even if the isotopic compositions in the fuel pin instances are identical (*e.g.*, fresh fuel at the beginning of life) since each instance may experience different spatial self-shielding effects and hence have different MGXS.

The degenerate scheme generates MGXS for each fuel pin instance using OpenMC's distributed cell tallies (Lax et al., 2014). The OpenCG region differentiation algorithm (Boyd et al., 2015) is used to build a new OpenMOC geometry with unique cells and materials for each fuel pin. The MGXS are appropriately selected from OpenMC's distributed cell tallies to populate the MGXS in the OpenMOC materials. Multi-group transport calculations with MGXS generated using null and degenerate schemes may be compared to quantify the impact of modeling spatial self-shielding effects in MGXS for fissile zones in heterogeneous geometries.

3. Test Cases

This paper models two test cases derived from the Benchmark for Evaluation And Validation of Reactor Simulations (BEAVRS) PWR model (Horelik et al., 2013). Each test case includes heterogeneous features – and corresponding spatial self-shielding effects – in order to understand their implications for accurate pin-wise MGXS generation. The impact of fuel enrichment, CRGTs, BPs, inter-assembly currents and water reflectors is considered. The geometric and material specifications for the two test cases are summarized in Sec. 3.1. The reference results computed with OpenMC for each of the test cases are discussed in Sec. 3.4.

-need to describe both pinwise fissoin rates and U-238 capture rates -latter papers can cite this one as reason to only analyze capture rates?

3.1. Benchmark Configurations

3.2. Single Fuel Assembly

3.3. Reflected Assembly Colorset

3.4. Verification Metrics

A series of OpenMC simulations were used to calculate reference eigenvalues, pin-wise fission rates, and pin-wise U-238 capture rates for both benchmarks. The ENDF/B-VII.1 continuous energy cross section libraries evaluated at 600K provided by the MCNP code (X-5 Monte Carlo Team, 2003) were used by OpenMC for all simulations. The reference solutions were computed with 100 inactive and 900 active batches of 10^7 particle histories per batch.

It should be noted that isotropic in lab scattering was employed for all reference calculations with OpenMC's "iso-in-lab" feature[2]. Although isotropic in lab scattering is a poor approximation for LWRs, it eliminated scattering source anisotropy as one possible cause of approximation error between OpenMC and OpenMOC in order to isolate approximation errors resulting from spatially self-shielded MGXS.

The reference eigenvalues are listed in Tab. 1. The OpenMC "combined" eigenvalue estimator is reported along with the associated 1-sigma uncertainty of one pcm for both test cases.

Table 1. Reference OpenMC eigenvalues for each test case.

Assembly	Colorset
0.99326 ± 0.00001	0.94574 ± 0.00001

[2]The OpenMC "iso-in-lab" feature samples the outgoing neutron energy from the scattering laws prescribed by the continuous energy cross section library, but the outgoing neutron direction of motion is sampled from an isotropic in lab distribution.

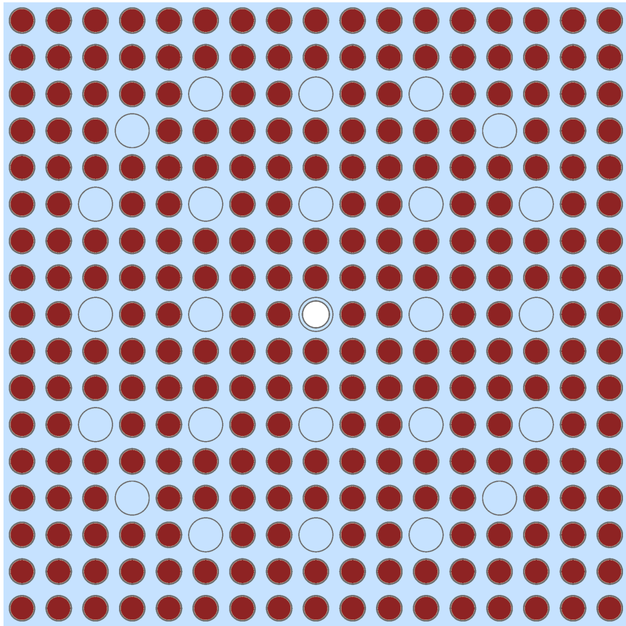

(a)

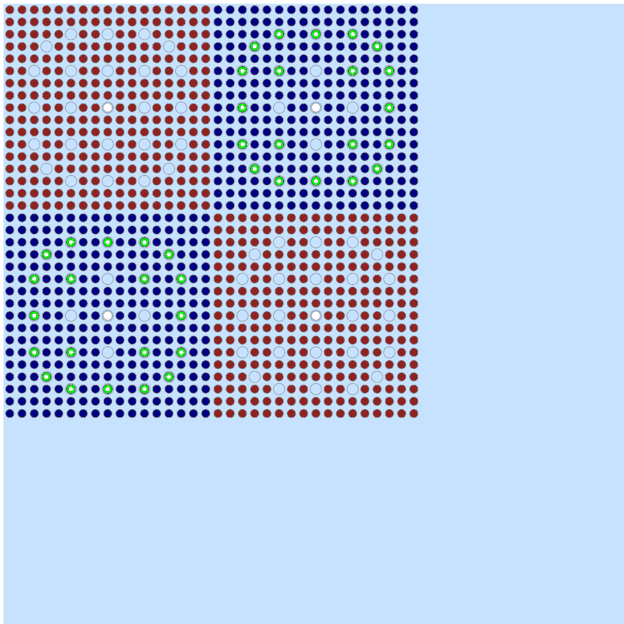

(b)

Figure 2. A (a) fuel assembly and (b) 2×2 assembly colorset with reflector.

The reference energy-integrated fission and U-238 capture rate spatial distributions were computed using rectilinear, pin-wise tally meshes in OpenMC and are shown in Fig. 3. The reaction rates were volume-integrated across each fuel pin. The fission rates include fission from only U-235 and U-238 for the fresh PWR UO_2 fuel. The reaction rates were normalized to the mean of all non-zero reaction rates in each benchmark. The reaction rates in the instrument tubes, CRGTs and BPs are all zero and are illustrated in white. The 1-sigma uncertainties are less than 0.08% in each pin for each benchmark.

As illustrated in the figures, the reaction rate rate distribu-

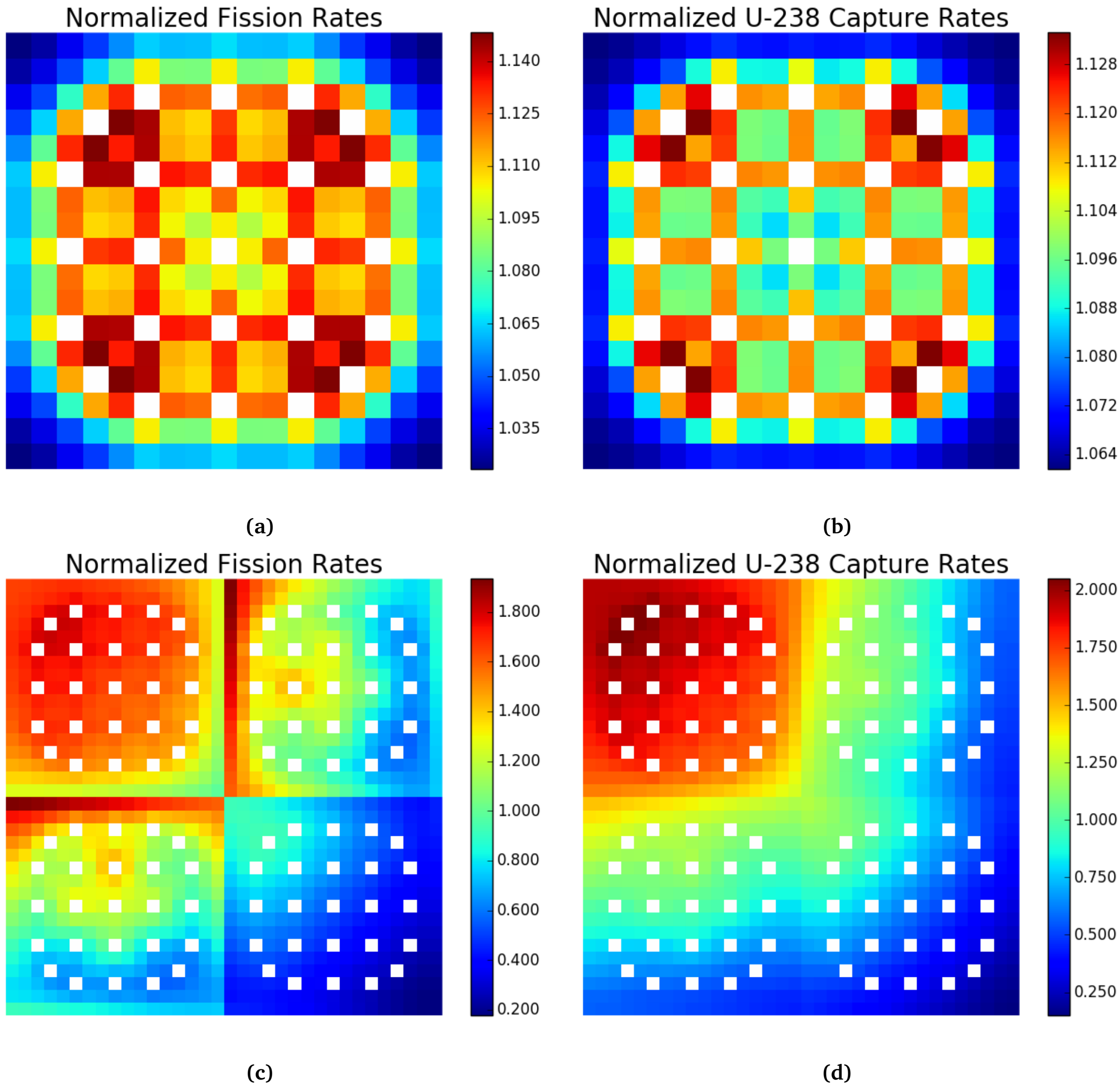

Figure 3. Fission and U-238 capture rates for the (a) – (b) assembly and (c) – (d) colorset.

tions are strongly dependent on the spatially heterogeneous features in each benchmark. For example, the CRGTs provide additional moderation and increase the fision and U-238 capture rates in nearby fuel pins. The inclusion of BPs reduces the neutron population and therefore the reaction rates for the surrounding fuel pins. The presence of a reflector with a mixture of vacuum and reflective BCs induces a tilt in the reaction rates across the assemblies in the colorset.

Although spatial heterogeneities generally have similar effects on both fission and U-238 capture rates, there are a few important differences to note. The U-238 capture rates in the assemblies are more sensitive than the fission rates to the spatial self-shielding induced by moderation in CRGTs. In addition, the capture rates in the colorset are more smoothly varying at the inter-assembly and assembly-reflector interfacea than the fission rates.

4. Results

4.1. Eigenvalues

In the results that follow, the bias $\Delta\rho$ compares the eigenvalue k_{eff}^{MOC} computed by OpenMOC to that of the reference eigenvalue k_{eff}^{MC} computed by OpenMC in units of pcm:

$$\Delta\rho = \left(k_{eff}^{MOC} - k_{eff}^{MC}\right) \times 10^5 \qquad (1)$$

Table 2. OpenMOC eigenvalue bias $\Delta\rho$.

Benchmark	Null	Degenerate
Assembly	-161	-161
Colorset	-142	-132

4.2. Fission Rates

-add figures of spatial distribution of errors -can I reproduce these plots? Do I have the batchwise.h5 results stored on my external hard drive??? If so, I should customize them for only 70 groups

Table 3. OpenMOC fission rate percent relative errors.

Benchmark	Metric	Null	Degenerate
Assembly	Max	0.380	0.315
	Mean	0.074	0.079
Colorset	Max	0.764	0.602
	Mean	0.178	0.138

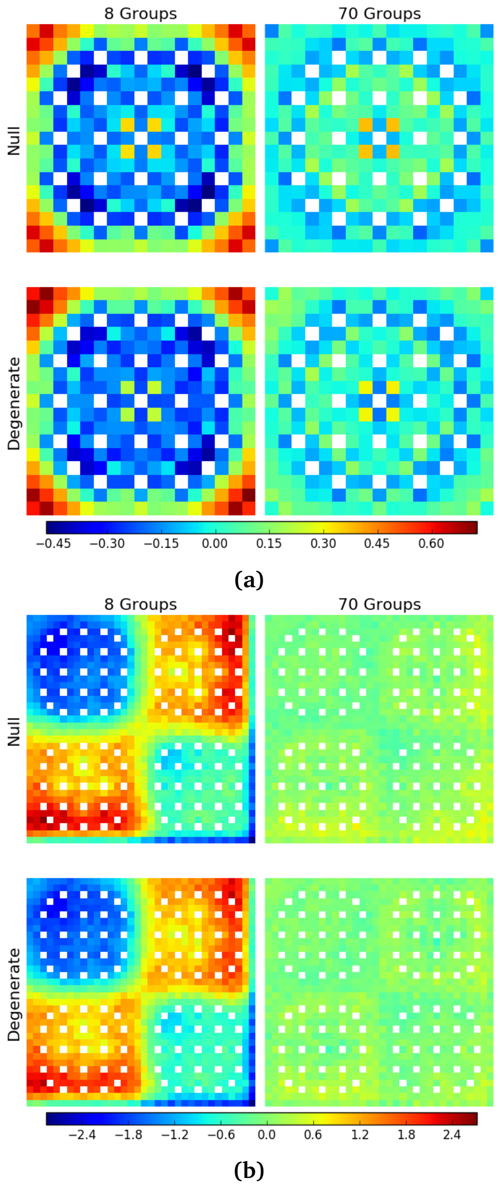

Figure 4. OpenMOC fission rate percent relative errors for the (a) assembly and (b) 2×2 colorset models.

4.3. Capture Rates

-add figures of spatial distribution of errors

Table 4. OpenMOC U-238 capture rate percent relative errors.

Benchmark	Metric	Null	Degenerate
Assembly	Max	-1.101	0.386
	Mean	0.479	0.086
Colorset	Max	-1.969	-0.783
	Mean	0.478	0.165

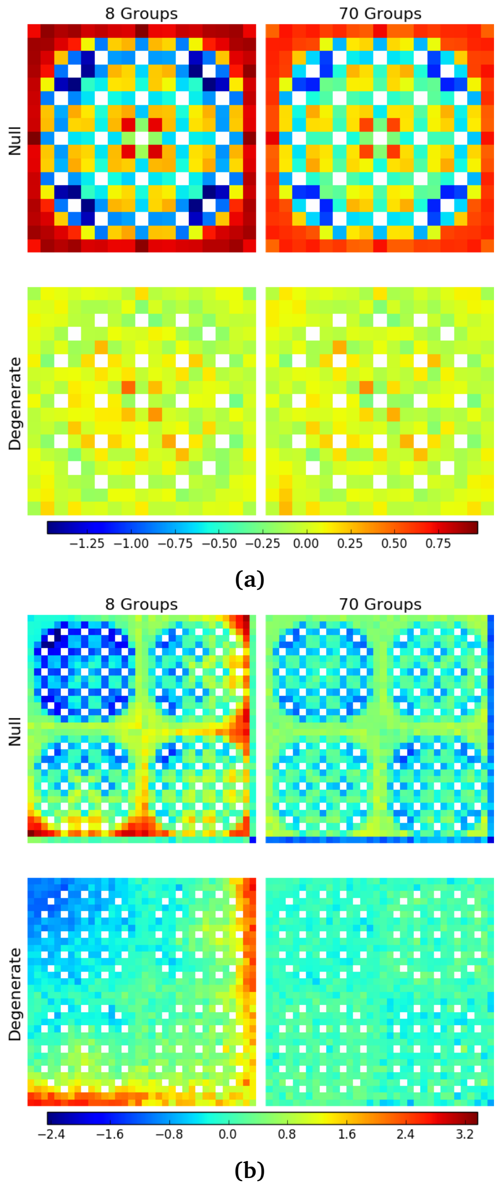

Figure 5. OpenMOC U-238 capture rate percent relative errors for the (a) assembly and (b) 2×2 colorset models.

5. Conclusions

Acknowledgments

This work was supported by the Idaho National Laboratory and the National Science Foundation Graduate Research Fellowship Grant No. 1122374. This research made use of the resources of the High Performance Computing Center at Idaho National Laboratory, which is supported by the Office of Nuclear Energy of the U.S. Department of Energy and the Nuclear Science User Facilities under Contract No. DE-AC07-05ID14517.

References

Boyd, W., Forget, B., Smith, K., 2015. OpenCG: A Combinatorial Geometry Modeling Tool for Data Processing and Code Verification. In: Int'l Conf. on Mathematics and Computational Methods Applied to Nuclear Science & Engineering. Nashville, TN, USA.

Boyd, W., Romano, P. K., Harper, S., 2016a. Equipping OpenMC for the Big Data Era. In: PHYSOR. Sun Valley, ID, USA.

Boyd, W., Shaner, S., Li, L., Forget, B., Smith, K., 2014. The OpenMOC Method of Characteristics Neutral Particle Transport Code. Annals of Nuclear Energy 68, 43–52.

Boyd, W., Siegel, A., He, S., Forget, B., Smith, K., 2016b. Parallel Performance Results for the OpenMOC Neutron Transport Code on Multicore Platforms. Int'l Journ. of High Performance Computing Applications.

Boyd, W. R. D., 2016. Reactor Agnostic Multi-Group Cross Section Generation for Fine-Mesh Deterministic Neutron Transport Simulations. Ph.D. thesis, Massachusetts Institute of Technology (submitted).

Cai, L., 2014. Condensation and Homogenization of Cross Sections for the Deterministic Transport Codes with Monte Carlo Method: Application to the GEN IV Fast Neutron Reactors. Ph.D. thesis, Université Paris Sud-Paris XI.

Horelik, N., Herman, B., Forget, B., Smith, K., 2013. Benchmark for Evaluation and Validation of Reactor Simulations (BEAVRS), v1.0.1. In: Int. Conf. Math. and Comp. Methods Applied to Nuc. Sci. & Eng. Sun Valley, Idaho, USA.

Lax, D., Boyd, W., Horelik, N., 2014. An Algorithm for Identifying Unique Regions in Constructive Solid Geometries. In: PHYSOR. Kyoto, Japan.

Leppänen, J., 2013. Serpent – A Continuous-Energy Monte Carlo Reactor Physics Burnup Calculation Code. VTT Technical Research Centre of Finland.

National Nuclear Data Center, Brookhaven National Laboratory, 2016. ENDF/B-VII.1 Evaluated Nuclear Data Library. http://www.nndc.bnl.gov/endf/b7.1/, accessed: 2016-08-09.

Nelson, A., 2014. Improved Convergence Rate of Multi-Group Scattering Moment Tallies for Monte Carlo Neutron Transport Codes. Ph.D. thesis, University of Michigan.

Redmond, E. L., 1997. Multi-Group Cross Section Generation via Monte Carlo Methods. Ph.D. thesis, Massachusetts Institute of Technology.

Rhodes, J., Smith, K., Lee, D., 2006. Casmo-5 development and applications. In: ANS Topical Meeting on Reactor Physics (PHYSOR). pp. 10–14.

Romano, P. K., Forget, B., 2013. The OpenMC Monte Carlo Particle Transport Code. Annals of Nuclear Energy 51, 274–281.

X-5 Monte Carlo Team, 2003. MCNP-A General Monte Carlo N-Particle Transport Code, Version 5. , Los Alamos National Laboratory.